Chemical Physics Letters 711 (2018) 127–131

Contents lists available at ScienceDirect

Chemical Physics Letters

journal homepage: www.elsevier.com/locate/cplett

Research paper

Resonance enhanced multiphoton ionization and mass analyzed threshold ionization spectroscopy of 4-fluorobenzonitrile

Yan Zhao[a], Yinghui Jin[a], Jiayu Hao[a], Yonggang Yang[a,b], Changyong Li[a,b,*], Suotang Jia[a,b]

[a] State Key Laboratory of Quantum Optics and Quantum Optic Devices, Institute of Laser Spectroscopy, Shanxi University, Taiyuan, Shanxi 030006, China
[b] Collaborative Innovation Center of Extreme Optics, Shanxi University, Taiyuan, Shanxi 030006, China

HIGHLIGHTS

- 2C REMPI and MATI spectra of 4-fluorobenzonitrile are obtained.
- Vibronic spectra of 4-fluorobenzonitrile in S_1 state are analyzed and assigned.
- Cationic vibrationic features of 4-fluorobenzonitrile are analyzed and assigned.
- Most of the active vibrations are related to the in-plane ring deformation.

ARTICLE INFO

Keywords:
4-fluorobenzonitrile
Two-color resonance enhanced multiphoton ionization
Mass-analyzed threshold ionization
Cationic spectra
Substitution effect

ABSTRACT

The vibrational features of 4-fluorobenzonitrile in the first electronically excited state S_1 and cationic ground state D_0 have been studied by two-color resonance enhanced multiphoton ionization and mass analyzed threshold ionization spectroscopy. Most of observed vibrations in the S_1 and D_0 states are related to in-plane ring deformation and CN bending motions. The band origin of the $S_1 \leftarrow S_0$ transition and adiabatic ionization energy of 4-fluorobenzonitrile are determined to be 36,616 ± 2 and 78,000 ± 5 cm^{-1}, respectively. These data provide insight into the substitution effect of fluorine atom and cyano group on the transition energy.

1. Introduction

Fluorinated organic molecules have been a subject of great interest due to their important applications in the agrochemical, medicinal, biological and material sciences [1–4]. In recent years, the chemical and physical properties of fluorinated aromatic compounds are investigated by various spectroscopic methods. The geometric changes of fluorination on fluorine-substituted compounds of benzene, benzonitrile, and pyridine have been studied by the high resolution microwave spectroscopy [5–7]. The vibrational features of fluorine-substituted derivatives of phenol, anisole, and aniline in the first electronically excited states S_1 and cationic ground states D_0 have also been studied by laser induced fluorescence (LIF), resonance enhanced multiphoton ionization (REMPI) and mass analyzed threshold ionization (MATI) spectroscopy [8–12]. Jiang and Levy performed the laser induced fluorescence and dispersed fluorescence experiments of 4-fluorobenzonitrile to analyze the internal vibration relaxation [13]. Arivazhagan et al. measured the vibrational properties of 4-fluorobenzonitrile in the electronic ground state S_0 by infrared and Raman spectroscopy [14]. To our best of knowledge, the detailed spectroscopic information of the S_1 and D_0 states of 4-fluorobenzonitrile are still unavailable in the literature.

In this paper, we study the two-color REMPI and MATI spectra of 4-fluorobenzonitrile. With the help of density functional theory (DFT) calculations, the active vibrations of 4-fluorobenzonitrile in the S_1 and D_0 states are assigned. The band origin of the $S_1 \leftarrow S_0$ transition and the adiabatic ionization energy are determined. Comparing these experimental data with those of benzonitrile and *para*-fluoro substituted derivatives provides a better understanding of the substitution effect of fluorine atom and cyano group on the transition energy.

2. Experimental and computational details

2.1. Experimental method

The experimental apparatus consists of a time-of-flight (TOF) mass spectrometer and two tunable UV lasers as described in previous publication [15]. The sample of 4-fluorobenzonitrile, purchased from

* Corresponding author at: Institute of Laser Spectroscopy, Shanxi University, Taiyuan, Shanxi 030006, China.
E-mail address: lichyong@sxu.edu.cn (C. Li).

https://doi.org/10.1016/j.cplett.2018.09.039
Received 15 August 2018; Accepted 15 September 2018
Available online 15 September 2018
0009-2614/

Sigma-Aldrich (99% purity) without further purification, was heated to 60 °C in order to obtain sufficient vapor pressure. A molecular beam was produced by expanding the vapor, seeded in 3 bar of argon, through a pulsed valve of 0.5 mm diameter nozzle into the vacuum. After passing through a 1 mm diameter skimmer, the molecular beam was crossed with the laser beams in the ionization region. The excitation and ionization lasers were generated by the frequency-doubled dye lasers (Sirah: CBR-D-24 and PrecisionScan-D), which were pumped by the third harmonics of two independent Nd:YAG lasers (Spectra Physics: INDI-40-10 and Quantel: Q-smart 850). The wavelengths of the dye lasers were calibrated using a wavemeter (HighFinesse WS-7). The REMPI spectrum was measured by scanning the excitation laser in the 260–274 nm range and fixing the ionization laser to 241 nm. The relative time between the two laser systems was controlled by a pulse delay generator (DG645) with 8 delay outputs.

For the MATI spectroscopy, molecules were excited to long-lived high n Rydberg states by the two tunable UV lasers. A weak pulse electric field of −1.3 V/cm was switched on about 200 ns after the laser pulses to reject the prompt ions. This field resulted in the lowering of ionization energy, which can be estimated by $4.0F^{1/2}$ cm^{-1} (F is electric field in unit of V/cm). After a time delay of 21 μs, a second pulse electric field of 140 V/cm was switch on to field-ionize the Rydberg neutrals. The produced threshold ions were accelerated and detected by a dual-stacked microchannel plates detector (Changcheng Microlight Equipment Co., 25 mm diameter) located at the end of a field-free flight tube. The mass spectra were collected and analyzed by a multichannel scaler (Stanford Research Systems, SR430), then transferred to a computer.

2.2. Computational method

In order to assign the observed bands in the REMPI and MATI spectra, we used the Gaussian 09 program package [16] to perform the geometry optimizations and frequency calculations of 4-fluorobenzonitrile. For the electronic ground state S_0 and the cationic ground state D_0, the density functional theory (DFT) calculations using the B3LYP functional were carried out with the 6-311 + + G (d,p) basis set. The first excited state S_1 was calculated using the time-dependent density functional theory (TDDFT) with the 6-311 + + G (d,p) basis set.

3. Results

3.1. Two-color REMPI spectrum of 4-fluorobenzonitrile

We recorded the vibronic spectrum of 4-fluorobenzonitrile in the S_1 state by two-color REMPI experiment. No fragments were observed in the mass spectrum. Fig. 1 displays the two-color REMPI spectrum of 4-fluorobenzonitrile near the origin of the $S_1 \leftarrow S_0$ transition. The result is in good agreement with the fluorescence excitation spectrum of 4-fluorobenzonitrile measured by Jiang and Levy [13]. The intense peak located at 36,616 cm^{-1} is assigned as the origin of the $S_1 \leftarrow S_0$ electronic transition. 4-fluorobenzonitrile is a planar molecule with 33 normal modes. Only the vibronic transitions with lager Franck-Condon factor can be observed in the REMPI spectrum [17,18]. Table 1 lists the frequencies of the observed vibronic bands of 4-fluorobenzonitrile, along with the computed values and their assignments. The assignments are based on the previous results [13] and our TDDFT calculation at B3LYP/6-311 + + G (d,p) level. The Varsanyi's numbering system [19] was adopted to approximately describe the normal modes of benzene-like vibrations, and the vibrational modes are expressed by Wilson's notation [20]. Most of active vibrations of 4-fluorobenzonitrile in the S_1 state are related to the in-plane deformation of aromatic ring. The pronounced bands at 145, 360, 497 and 1176 cm^{-1} are assigned to the transitions of 15_0^1, $6a_0^1$, $6b_0^1$, and 13_0^1, respectively. Modes 6a and 6b mainly involve the in-plane deformation of aromatic ring. Modes 15 and 13 are related to the substitute-sensitive in-plane ring-CN bending and ring-CN stretching vibrations, respectively. The bands at 792 and 1586 cm^{-1} result from the ring breathing vibration 1^1 and its overtone 1^2. The out-of-plane ring deformation vibration 4^1 appears at 506 cm^{-1}. The weak band at 597 cm^{-1} corresponds to CN in-pline bending β(CN). The high-frequency bands at 1151 and 1288 cm^{-1} are assigned to the combination vibrations $6a^1 1^1$ and $6b^1 1^1$, respectively.

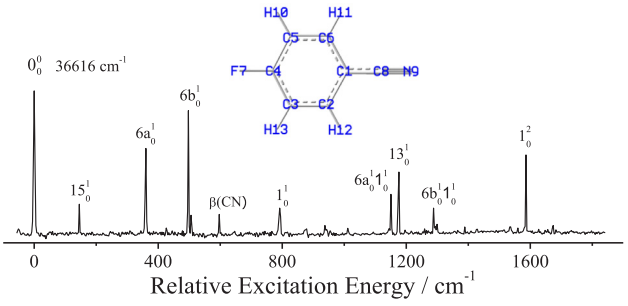

Fig. 1. Two-color REMPI spectrum of 4-fluorobenzonitrile obtained by fixing the ionization laser at 241 nm and scanning the excitation laser. The spectrum is shifted by 36,616 cm^{-1}. The insert shows the molecular structure and atom labels.

Table 1
Observed vibrational frequencies (cm^{-1}) of 4-fluorobenzonitrile in two-color REMPI spectrum and their assignments.[a] The predicted values obtained from the TD-B3LYP/6-311G + + (d,p) calculation are scaled by 0.9766.

Ref. [34]	This work			Assignment[b]
	Exp. [a]	Exp. Rel. Int.	Cal.	
	0	100		0_0^0, band origin
	145	22	151	15_0^1, β(C-CN)
	360	61	350	$6a_0^1$,β(CCC)
497	497	86	496	$6b_0^1$,β(CCC)
	506	15	523	4_0^1, γ(CCC), γ(C-F)
	597	15	608	β(CN)
792	792	20	792	1_0^1, breathing
	878	5		$6a_0^1 4_0^1$
	938	8		$15_0^1 1_0^1$
	1011	6		4_0^2
	1151	29		$6a_0^1 1_0^1$
1176	1176	44	1186	13_0^1, ν(C-CN)
	1288	20		$6b_0^1 1_0^1$
	1299	9	1302	$18b_0^1$, β(CH)
1588	1586	56	1584	1_0^2
	1674	8		$6b_0^1 13_0^1$

[a] The experimental values are shifts from 36,616 cm^{-1}.
[b] ν, stretching; β, in-plane bending; γ, out-of-plane bending.

3.2. PIE and MATI spectra of 4-fluorobenzonitrile

The photoionization efficiency (PIE) and MATI experiments are performed to determine the adiabatic ionization energy (IE) of 4-fluorobenzonitrile. The PIE curve (available on request) recorded by ionizing via the $S_1 0^0$ intermediate state indicates the IE of 4-fluorobenzonitrile to be 78,000 cm^{-1} with an uncertainty of 10 cm^{-1}. Because the MATI experiment only detects the threshold ions resulting from the field ionization of the high Rydberg molecules, it leads to a sharp peak at the ionization limit and yields a more precise IE. Figs. 2 and 3 show the MATI spectra of 4-fluorobenzonitrile recorded via the 0^0, 15^1, $6a^1$, $6b^1$, β(C-CN), and 1^1 levels of the S_1 state. The most intense band 0^+ in Fig. 2a corresponds to the origin of the transition $D_0 \leftarrow S_1$. The resulting adiabatic IE, including the correction for Stark effect due to the pulsed electronic field, is determined to be

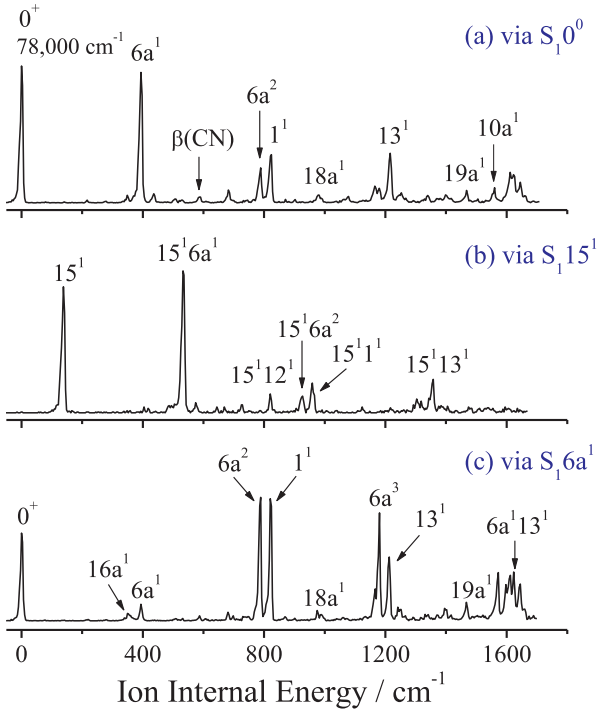

Fig. 2. MATI spectra of 4-fluorobenzonitrile recorded via (a) $S_1 0^0$, (b) $S_1 15^1$, and (c) $S_1 6a^1$ intermediate states.

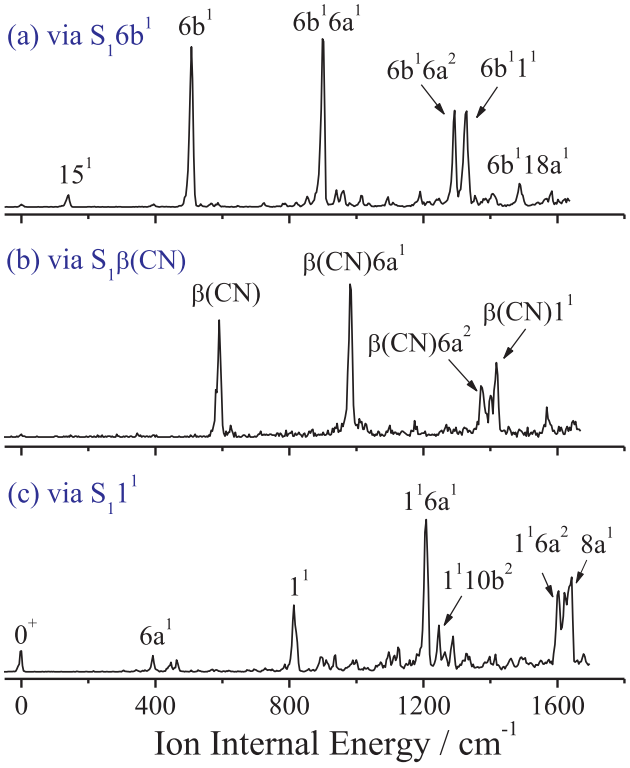

Fig. 3. MATI spectra of 4-fluorobenzonitrile recorded via (a) $S_1 6b^1$, (b) $S_1\beta(CN)$, and (c) $S_1 1^1$ intermediate states.

78,000 ± 5 cm^{-1} (9.6708 ± 0.0006 eV). This result is in agreement with that measured one by our PIE experiment. Comparison with the previously reported IE value of 9.74 eV by Palmer et al. on the basis of the photoelectron spectroscopy [21], the MATI experiment provides a more precise value of IE.

Table 2
Observed vibrational frequencies (cm^{-1}) in the MATI spectra of 4-fluorobenzonitrile and their assignments.[a] The predicted values obtained from the B3LYP/6-311G++(d,p) calculation are scaled by 0.9856.

Intermediate level in the S_1 state						Cal.	Assignment[b]
0^0	15^1	$6a^1$	$6b^1$	β(CN)	1^1		
	139		141			150	15^1, β(C-CN)
348		350				358	$16a^1$, γ(CCC)
394		394			393	400	$6a^1$, β(CCC)
436					446	444	$10b^2$
					463		$11^1 6a^1$
			508			532	$6b^1$, β(CCC)
	533						$15^1 6a^1$
	574						$15^1 10b^2$
587				590		598	β(CN)
				624			$10b^1 6a^1$
682		681				684	12^1, β(CCC)
	725						15^1β(CN)
789		789					$6a^2$
	821						$15^1 12^1$
822		820			813	819	1^1, breathing
					895		$1^1 11^1$
			899				$6b^1 6a^1$
	927						$15^1 6a^2$
			940		937		$6b^1 10b^2$
	959		961				$15^1 1^1$
978		975				972	$18a^1$
				981			β(CN) $6a^1$
			1014				$6b^2$
1078							$6a^1 12^1$
			1094	1100	1097		β(CN) $6b^1$
					1124	1120	14^1, β(CH)
1166						1169	$9a^1$, β(CH)
				1174			β^2(CN)
1180		1180					$6a^3$
			1190				$6b^1 12^1$
					1208		$1^1 6a^1$
1216		1213				1224	13^1, ν(C-CN)
					1246		$1^1 10b^2$
1253		1252					β(CN)12^1
			1293		1289		$6b^1 6a^2$
	1303						$15^1 9a^1$
			1329		1327		$6a^1 1^1$
	1358						$15^1 13^1$
				1371			β(C-CN)$6a^2$
			1407				$6b^2 6a^1$
				1418	1415		β(CN)1^1
1468		1467				1469	$19a^1$, ν(CC), ν(C-F)
			1486				$6b^1 18a^1$
1560						1567	$10a^1$, γ(CH)
				1568			β(CN)$18a^1$
		1573					$6a^4$
			1583				$6b^1 6a^1 12^1$
1612		1612			1603		$1^1 6a^2$
					1621		1^2
1623		1623					$6a^1 13^1$
1645		1645			1642	1640	$8a^1$, ν(CC)

[a] The experimental values are shifts from 78,000 cm^{-1}.
[b] ν, stretching; β, in-plane bending; γ, out-of-plane bending.

The measured vibrational frequencies of 4-fluorobenzonitrile in the D_0 state are also summarized in Table 2 together with the calculated frequencies and possible assignments. When the $S_1 0^0$ is used as the intermediate state, the intense transitions at 394, 789, 824, and 1216 cm^{-1} are assigned to the in-plane ring deformation vibrations $6a^1$, $6a^2$, 1^1 and 13^1 of 4-fluorobenzonitrile cation, respectively. The weak bands at 587 cm^{-1} results from the in-plane CN bending vibration β(CN). In Fig. 2b, when the $S_1 15^1$ is used as intermediate state, the MATI spectrum displays a strong band at 139 cm^{-1} corresponding to the cationic vibration 15^1 with the same vibrational pattern as the intermediate state, and other four strong MATI bands at 533, 927, 959 and 1358 cm^{-1} are tentatively assigned to the combination bands $15^1 6a^1$, $15^1 6a^2$, $15^1 1^1$ and $15^1 13^1$, respectively. Therefore, the

Table 3
Calculated and measured geometrical parameters of 4-fluorobenzonitrile in the S_0, S_1 and D_0 states.

	Exp.[a]	S_0[b]	S_1[c]	D_0[b]	$\Delta(S_1\text{-}S_0)$	$\Delta(D_0\text{-}S_1)$
Bond length (Å)						
$C_1\text{-}C_2$	1.400	1.403	1.434	1.436	0.031	0.002
$C_2\text{-}C_3$	1.377	1.389	1.423	1.366	0.034	−0.057
$C_3\text{-}C_4$	1.378	1.388	1.408	1.420	0.020	0.012
$C_4\text{-}C_5$	1.375	1.388	1.408	1.420	0.020	0.012
$C_5\text{-}C_6$	1.379	1.389	1.423	1.366	0.034	−0.057
$C_6\text{-}C_1$	1.400	1.403	1.434	1.436	0.031	0.002
$C_4\text{-}F_7$	1.364	1.349	1.342	1.300	−0.007	−0.042
$C_1\text{-}C_8$	1.445	1.431	1.404	1.403	−0.027	−0.001
$C_8\text{-}N_9$	1.143	1.156	1.165	1.164	0.009	−0.001
Angle(deg)						
$C_1C_2C_3$	119.9	120.2	119.4	119.5	−0.8	0.1
$C_2C_3C_4$	118.6	118.6	118.1	118.0	−0.5	−0.1
$C_3C_4C_5$	123.0	122.6	124.0	123.8	1.4	−0.2
$C_4C_5C_6$	118.7	118.6	118.1	118.0	−0.5	−0.1
$C_5C_6C_1$	119.8	120.2	119.4	119.5	−0.8	0.1
$C_6C_1C_2$	120.0	119.9	120.8	121.2	0.9	0.4

[a] Experimental data from Reference [22].
[b] B3LYP/6-311G++(d,p) calculation.
[c] TD-B3LYP/6-311G++(d,p) calculation.

spectrum has a similar profile as the MATI spectrum via the $S_1 0^0$ intermediate state. This similarity can be also observed in the MATI spectra via the $6b^1$, β(CN), and 1^1 vibrations of the S_1 state, as shown in Fig. 3. The MATI spectrum via $S_1 6a^1$ intermediate state is presented in Fig. 2c. A weak transition at 394 cm^{-1} is assigned to mode 6a, and the intense peaks at 789, 820, 1180, 1213, 1623 cm^{-1} to the vibrations $6a^2$, 1^1, $6a^3$, 13^1, and $6a^1 13^1$, respectively.

4. Discussion

4.1. Structure and vibrations of 4-fluorobenzonitrile in S_1 and D_0 states

The molecular structure and atom labels of 4-fluorobenzonitrile are showed in the inset of Fig. 1. Table 3 lists the calculated geometrical parameters of 4-fluorobenzonitrile in the neutral ground S_0, first excited S_1 and cationic ground D_0 states. For the S_0 state, it is obvious that the theoretical bond lengths and bond angles are in good agreement with the experimental values measured by the X-ray crystallography [22]. During the $S_1 \leftarrow S_0$ transition, the C-C bond lengths of the aromatic ring increase by 0.028 Å on average, whereas the $C_1\text{-}C_8$ and $C_4\text{-}F_7$ bond lengths decrease. The bond angles of $\angle C_6C_1C_2$ and $\angle C_3C_4C_5$ associated with substitutions also increase. On the basis of TDDFT calculation, the first excited state S_1 has a $\pi\pi^*$ character, which is dominated by the LUMO ← HOMO transition. These structural changes upon electronic excitation result from the π electron excitation of aromatic ring and the decrease of electron density on cyano group and fluorine atom. Thus, the observed vibrations in the REMPI spectrum of 4-fluorobenzonitrile are mainly associated with the in-plane ring deformation modes 6a, 6b, 13 and 1^2 and in-plane CN bending vibration β(CN). In previous studies on benzonitrile [23], 4-fluorophenol [12], and 4-chloroanisole [24], similar geometrical changes are also been observed.

According to the natural population analysis (NPA), the $D_0 \leftarrow S_1$ ionization process of 4-fluorobenzonitrile mainly involves the removal of the π^* electron on the aromatic ring. The resulting major changes of molecular structure are the decrease of the $C_2\text{-}C_3$, $C_5\text{-}C_6$ and $C_4\text{-}F_7$ bond lengths, which indicates a small shrinkage in size of aromatic ring upon ionization. Thus, it leads to a remarkable change in the vibrational frequencies. The measured frequencies of in-plane ring deformation modes 6a, 6b, and 1 are 360, 497, and 792 cm^{-1} in the S_1 state, and 394, 508, and 820 cm^{-1} in the D_0 state. It is obvious that these vibrational frequencies in the D_0 state are higher than ones in the S_1 state. Because the vibrational frequency reflects the rigidity of the chemical bond related to the vibration, the increase of the vibrational frequencies suggests that the bond strength of the ring is stronger in the D_0 state than in the S_1 state.

4.2. Excitation and ionization energies of 4-fluorobenzonitrile

It is known that the interactions between the substituent and the aromatic ring involve the conjugation (resonance) effect through the π orbital and the inductive effect through σ bond [9]. The collective effect can cause a change on the electron density around the aromatic ring, and gives rise to a decrease in the zero-point energy (ZPE) level of electronic state. If the magnitude of the decrease in the ZPE level of the upper electronic state is greater than that in the lower electronic state, it leads to a red shift in the transition energy. Conversely, it causes a blue shift in the transition energy.

Table 4 lists the excitation energies of $S_1 \leftarrow S_0$ transition and adiabatic IEs of phenol [25], anisole [26], aniline [27], benzonitrile [28] and their *para*-fluoro substituted derivatives from the LIF, REMPI, MATI, and ZEKE spectroscopy [9,10,27,29]. The E_1 of 4-fluorophenol, 4-fluoroanisole, and 4-fluoroaniline are red-shifted by 1232, 1237, and 1377 cm^{-1} with respect to phenol, anisole, and aniline, respectively.

Table 4
Measured transition energies (cm^{-1}) of phenol, anisole, aniline, benzonitrile, and their their *para*-fluoro substituted derivatives.[a]

Molecule	$E_1(S_1 \leftarrow S_0)$	ΔE_1	$E_2(D_0 \leftarrow S_1)$	ΔE_2	IE	ΔIE
Phenol[b]	36,349	0	32,276	0	68,625	0
4-Fluorophenol[c]	35,117	−1232	33,460	1184	68,577	-48
Anisole[d]	36,383	0	30,016	0	66,399	0
4-Fluoroanisole[e]	35,146	−1237	31,291	1275	66,437	38
Aniline[f]	34,029	0	28,242	0	62,271	0
4-Fluoroaniline[f]	32,652	−1377	29,891	1649	62,543	272
Benzonitrile[g]	36,518	0	41,972	0	78,490	0
4-Fluorobenzonitrile[h]	36,616	98	41,384	−588	78,000	−490
4-Methylbenzonitrile[i]	36,222	−296	38,933	−3039	75,155	−2845

[a] ΔE_1, ΔE_2, and ΔIE are shifts of E_1, E_2 and IE with respect to phenol, anisole, aniline, and benzonitrile.
[b] Reference [25].
[c] Reference [9].
[d] Reference [26].
[e] Reference [10].
[f] Reference [27].
[g] Reference [28].
[h] This work.
[i] Reference [29].

The previous studies reported that the red shift probably result from the dominant conjugation effect upon $S_1 \leftarrow S_0$ transition [8,24,30]. When the CH_3 substituent locates at the *para* position on the aromatic ring of the benzonitrile, 4-methylbenzonitrile also shows a red shift in the E_1 due to the dominant conjugation effect. Inversely, the E_1 of 4-fluorobenzonitrile is slightly greater than that of benzonitrile. This blue shift in the E_1 for 4-fluorobenzonitrile indicates that the inductive effect is likely dominant during $S_1 \leftarrow S_0$ transition. Similar observations also are found for the molecules 2-fluorophenol, 3-fluorophenol, 2-fluoroaniline, 2-fluoroanisole, and 3-fluoroanisole [10,31,32].

As shown in Table 4, the E_2 of 4-fluorophenol, 4-fluoroanisole, and 4-fluoroaniline are greater than those of phenol, anisole, and aniline by 1184, 1275, and 1649 cm^{-1}, respectively. Because the $D_0 \leftarrow S_1$ process involves the removal of one electron, the blue shift indicates that the substitution of fluorine atom causes a slight decrease in the electron density around the aromatic ring [8,10,27]. Therefore, fluorine atom plays an electron-withdrawing role in this process. In contrast, the E_2 of 4-methylbenzonitrile and 4-fluorobenzonitrile are less than that of benzonitrile by 588 and 3039 cm^{-1}, respectively. This red shift indicates that fluorine atom and CH_3 group increase the electron density near the ring. Fluorine atom shows the same substitution effect as CH_3 group and plays an electron-donating role in the $D_0 \leftarrow S_1$ transition. So it can be seen that fluorine atoms play two different roles in different molecules. This can be also observed for chlorine in the chlorobenzene and 3-chlorostyrene [33]. These results suggest that the energy shift of electronic transition is associated with the nature of substituents as well as parent molecules.

As for substitution effect on ionization energy, generally, the electron-donating group reduces the IE of the parent molecule, and the electron-withdrawing group increases the IE. The OH, OCH_3, and NH_2 groups are regarded as the electron-donating groups, whereas the CN is the electron-withdrawing group. As a result, the IE of 4-fluorobenzonitrile is higher than those of 4-fluorophenol, 4-fluoroanisole, and 4-fluoroaniline, as showed in Table 4.

5. Conclusion

We have applied the two-color REMPI and MATI spectroscopy to record the vibrational features of 4-fluorobenzonitrile in the S_1 and D_0 states. The band origin of the $S_1 \leftarrow S_0$ electronic transition and adiabatic ionization energies of 4-fluorobenzonitrile in the gas phase are determined to be 36,616 ± 2 and 78,000 ± 5 cm^{-1}, respectively. The observed vibrations of 4-fluorobenzonitrile in the S_1 and D_0 states are mainly related to the in-plane ring deformation and in-plane CN bending vibrations. Their vibrational frequencies in the D_0 state are greater than in the S_1 state. The *para*-fluoro substitution on benzonitrile leads to a blue shift in the E_1 and a red shift in the E_2. These results suggest that the inductive effect may be dominant in the $S_1 \leftarrow S_0$ transition, and fluorine atom plays an electron-donating role in the $D_0 \leftarrow S_1$ ionization process.

Acknowledgments

This work was supported by the National Key R&D Program of China (Grant No. 2017YFA0304203), PCSIRT (No. IRT_17R70), National Natural Science Foundation of China (Grants Nos. 61575115, 61378039, 11434007), 111 project (Grant No. D18001), the Construction of State Key Laboratory of Quantum Optics and Quantum Optics Devices, China (Grant No. 2015012001-20), and Fund for Shanxi"1331 Project" Key Subjects Construction.

References

[1] J. Peter, The unique role of fluorine in the design of active ingredients for modern crop protection, ChemBioChem 5 (2004) 570–589.
[2] K. Müller, C. Faeh, F. Diederich, Fluorine in pharmaceuticals: looking beyond intuition, Science 317 (2007) 1881.
[3] R. Berger, G. Resnati, P. Metrangolo, E. Weber, J. Hulliger, Organic fluorine compounds: a great opportunity for enhanced materials properties, Chem. Soc. Rev. 40 (2011) 3496–3508.
[4] S.M. Ametamey, M. Honer, P.A. Schubiger, Molecular imaging with PET, Chem. Rev. 108 (2008) 1501–1516.
[5] M. Kamaee, M. Sun, H. Luong, J. van Wijngaarden, Investigation of structural trends in mono-, di-, and pentafluorobenzonitriles using Fourier transform microwave spectroscopy, J. Phys. Chem. A 119 (2015) 10279–10292.
[6] W. Sun, I.B. Lozada, J. van Wijngaarden, Fourier transform microwave spectroscopic and *ab initio* study of the rotamers of 2-fluorobenzaldehyde and 3-fluorobenzaldehyde, J. Phys. Chem. A 122 (2018) 2060–2068.
[7] W. Sun, J. van Wijngaarden, Structural elucidation of 2-fluorothiophenol from Fourier transform microwave spectra and *ab initio* calculations, J. Mol. Struct. 1144 (2017) 496–501.
[8] J. Huang, K. Huang, S. Liu, Q. Luo, W. Tzeng, Vibrational spectra and theoretical calculations of *p*-chlorophenol in the electronically excited S_1 and ionic ground D_0 states, J. Photochem. Photobiol. A Chem. 193 (2008) 245–253.
[9] B. Zhang, C. Li, H. Su, J.L. Lin, W.B. Tzeng, Mass analyzed threshold ionization spectroscopy of *p*-fluorophenol cation and the p-fluoro substitution effect, Chem. Phys. Lett. 390 (2004) 65–70.
[10] K.S. Shiung, D. Yu, S.Y. Tzeng, W.B. Tzeng, Cation spectroscopy of *o*-fluoroanisole and *p*-fluoroanisole by two-color resonant two-photon mass-analyzed threshold ionization, Chem. Phys. Lett. 524 (2012) 38–41.
[11] W.C. Peng, P.Y. Wu, S.Y. Tzeng, W.B. Tzeng, Resonant two-photon ionization and mass-analyzed threshold ionization spectroscopy of 3,5-difluorophenol, Chem. Phys. Lett. 700 (2018) 145–148.
[12] C. Ratzer, M. Nispel, M. Schmitt, Structure of 4-fluorophenol and barrier to internal –OH rotation in the S_1-state, Phys. Chem. Chem. Phys. 5 (2003) 812–819.
[13] S. Jiang, D.H. Levy, Supersonic jet studies on the photophysics of substituted benzenes and naphthalenes, J. Phys. Chem. A 106 (2002) 8590–8598.
[14] M. Arivazhagan, R. Meenakshi, S. Prabhakaran, Vibrational spectroscopic investigations, first hyperpolarizability, HOMO–LUMO and NMR analyzes of *p*-fluorobenzonitrile, Spectrochim. Acta A Mol. Biomol. Spectrosc. 102 (2013) 59–65.
[15] Y. Jin, Y. Zhao, Y. Yang, L. Wang, C. Li, S. Jia, Two-color resonance enhanced multi-photon ionization and mass analyzed threshold ionization spectroscopy of 2-amino-benzonitrile and the CN substitution effect, Chem. Phys. Lett. 692 (2018) 395–401.
[16] M.J. Frisch, G.W. Trucks, H.B. Schlegel, G.E. Scuseria, M.A. Robb et al. Gaussian 09, Revision C.01,. Gaussian, Inc., Wallingford CT, 2009.
[17] S. Schumm, M. Gerhards, K. Kleinermanns, Franck – Condon simulation of the $S_1 \rightarrow S_0$ spectrum of phenol, J. Phys. Chem. A 104 (2000) 10648–10655.
[18] J. Bloino, M. Biczysko, O. Crescenzi, V. Barone, Integrated computational approach to vibrationally resolved electronic spectra: anisole as a test case, J. Chem. Phys. 128 (2008) 244105.
[19] G. Varsanyi, Assignments of Vibrational Spectra of Seven Hundred Benzene Derivatives, Wiley, New York, 1974.
[20] E.B. Wilson, The normal modes and frequencies of vibration of the regular plane hexagon model of the benzene molecule, Phys. Rev. 45 (1934) 706–714.
[21] M.H. Palmer, W. Moyes, M. Spiers, The electronic structure of substituted benzenes: ab initio calculations and photoelectron spectra for benzonitrile, the tolunitriles, fluorobenzonitriles, dicyanobenzenes and ethynylbenzene, J. Mol. Struct. 62 (1980) 165–187.
[22] D. Britton, W.B. Gleason, *p*-Fluorobenzonitrile, Acta Crystallogr. Sect. B: Struct. Sci. Cryst. Eng. Mat. 33 (1977) 3926–3928.
[23] R.M. Helm, H.P. Vogel, H.J. Neusser, Highly resolved UV spectroscopy: structure of S_1 benzonitrile and benzonitrile-argon by correlation automated rotational fitting, Chem. Phys. Lett. 270 (1997) 285–292.
[24] D. Yu, C. Dong, M. Cheng, L. Hu, Y. Du, Q. Zhu, C. Zhang, Resonance-enhanced multi-photon ionization (REMPI) spectroscopy of the ^{35}Cl and ^{37}Cl isotopomers of *p*-chloroanisole, J. Mol. Spectrosc. 265 (2011) 86–91.
[25] O. Dopfer, K. Müller-Dethlefs, S_1 excitation and zero kinetic energy spectra of partly deuterated 1:1 phenol–water complexes, J. Chem. Phys. 101 (1994) 8508–8516.
[26] M. Pradhan, C. Li, J.L. Lin, W.B. Tzeng, Mass analyzed threshold ionization spectroscopy of anisole cation and the OCH_3 substitution effect, Chem. Phys. Lett. 407 (2005) 100–104.
[27] J.L. Lin, W.B. Tzeng, Mass analyzed threshold ionization of deuterium substituted isotopomers of aniline and *p*-fluoroaniline: isotope effect and site-specific electronic transition, J. Chem. Phys. 115 (2001) 743–751.
[28] M. Araki, S. Sato, K. Kimura, Two-color zero kinetic energy photoelectron spectra of benzonitrile and its van der Waals complexes with argon. Adiabatic ionization potentials and cation vibrational frequencies, J. Phys. Chem. 100 (1996) 10542–10546.
[29] K. Suzuki, S. Ishiuchi, M. Sakai, M. Fujii, Pulsed field ionisation - ZEKE photoelectron spectrum of *o*-, *m*- and *p*-tolunitrile, J. Electron. Spectrosc. Relat. Phenom. 142 (2005) 215–221.
[30] J. Huang, J.L. Lin, W.B. Tzeng, Mass analyzed threshold ionization spectroscopy of the ^{35}Cl and ^{37}Cl isotopomers of *p*-chlorophenol and isotope effect, Chem. Phys. Lett. 422 (2006) 271–275.
[31] L. Yuan, C. Li, J.L. Lin, S.C. Yang, W.B. Tzeng, Mass analyzed threshold ionization spectroscopy of *o*-fluorophenol and *o*-methoxyphenol cations and influence of the nature and relative location of substituents, Chem. Phys. 323 (2006) 429–438.
[32] K.S. Shiung, D. Yu, H.C. Huang, W.B. Tzeng, Rotamers of *m*-fluoroanisole studied by two-color resonant two-photon mass-analyzed threshold ionization spectroscopy, J. Mol. Spectrosc. 274 (2012) 43–47.
[33] C. Dong, L. Zhang, S. Liu, L. Hu, M. Cheng, Y. Du, Q. Zhu, C. Zhang, REMPI and MATI spectroscopic study of selected *cis* and *trans* 3-chlorostyrene rotamers, J. Mol. Spectrosc. 292 (2013) 35–46.
[34] C.H. Kwon, H.L. Kim, M.S. Kim, Vibrational analysis of vacuum ultraviolet mass-analyzed threshold ionization spectra of phenylacetylene and benzonitrile, J. Phys. Chem. A 107 (2003) 10969–10975.